Supplement of Atmos. Chem. Phys., 18, 5607–5617, 2018
https://doi.org/10.5194/acp-18-5607-2018-supplement

Atmospheric Chemistry and Physics
Open Access
EGU

Supplement of

Sources and oxidative potential of water-soluble humic-like substances ($HULIS_{WS}$) in fine particulate matter ($PM_{2.5}$) in Beijing

Yiqiu Ma et al.

Correspondence to: Xinghua Qiu (xhqiu@pku.edu.cn) and Di Hu (dihu@hkbu.edu.hk)

Content of this file

Section S1. HPLC-ELSD analysis of $HULIS_{WS}$ mass concentration.

$HULIS_{WS}$ mass concentration was analyzed by a high-performance liquid chromatography system (HPLC, ThermoFisher Scientific, Waltham, MA, USA) coupled with an evaporative light scattering detector (Alltech ELSD 3300, Grace, Houston, TX, USA). Detailed method was provided in Lin et al. (2010) Since there is no requirement for further separation, a polyaryletheretherketone tube (15 m, 0.127 mm i.d., Alltech, Dearfield, IL, USA) instead of the analytical column was used to connect the HPLC injector port and ELSD). $HULIS_{WS}$ was eluted by isocratic elution with acetonitrile: distilled deinoized water (1:4, vol/vol) at a rate of 0.6 mL min^{-1}. The ELSD was operated at a N_2 flow rate of 1.5 L min^{-1} and a drift tubing temperature of 90°C. The recoveries of representative $HULIS_{WS}$ species were provided in Lin et al. (2010)

Section S2. GC-MS analysis of individual $HULIS_{WS}$ species.

Individual $HULIS_{WS}$ species were analyzed using gas chromatography-mass spectrometry (GC-MS; Agilent 7890A-5975C, Santa Clara, CA, USA) in electron ionization (EI) mode. A HP-5MS column (30 m, 250 μm i.d., 0.25 μm film thickness, Agilent, Santa Clara, CA, USA) was used to separate individual species. Two microliter of sample was injected into GC in splitless mode. The GC oven temperature program was set as follows: held at 80°C for 5 min; 3°C min^{-1} to 200°C and held for 2 min; 15°C min^{-1} to 300°C and held for 15 min. For most compounds with authentic standards, they were identified and quantified by comparison to the standards. For terephthalic acid, 2-hydroxybenzoic acid, and 1,2,3-/1,2,4-benzenetricarboxylic acids, which were lack of authentic standards, isophthalic acid, 3-hydroxybenzoic acid, and 1,3,5-benzenetricarboxylic acid were used as the surrogate compounds for calibration and recovery test, respectively. Similarly, for SOA markers, surrogate compounds with similar functional groups were used for calibration and they were determined following the procedure described in Hu et al. (2008). Recoveries for all measured species were within 72%-106%.

Section S3. Positive Matrix Factorization (PMF) analysis.

PMF is a widely used receptor model for the source apportionment of fine particulate matter ($PM_{2.5}$). In this model, the original data matrix X could be divided into a factor contribution matrix G and a factor profile matrix F:

$$\underset{m\times n}{X} = \underset{m\times p}{G} \times \underset{p\times n}{F} + \underset{m\times n}{\varepsilon}$$

where n stands for the sample number, m stands for the species number, p refers to the number of factors in PMF solution, ε refers to a residual matrix.

During calculation, the sum of scaled residual Q was minimized:

$$Q = \sum_{i=1}^{m}\sum_{j=1}^{n}\left(\frac{e_{ij}}{\sigma_{ij}}\right)^2$$

where e_{ij} is the residual of each sample, and σ_{ij} is the uncertainty of the j^{th} species for the sample i.

In this study, a total of 66 samples and 13 species was included in the final PMF solution. The uncertainty setting was referred to Hu et al. (2010). Briefly, the uncertainties of $HULIS_{WS}$ mass concentration, extrinsic DTT activity (DTT_V), major ions (Mg^{2+}, Ca^{2+}, NH_4^+, SO_4^{2-}, and nss-Cl^-), SOA marker (MonoT) and individual $HULIS_{WS}$ species (4M5NC, 3M6NC, 123Ben, 124Ben, and TPha) were set as 0.4 of average annual value. Hopane and Levoglucosan (LevoG) were set as 0.2 of average annual value. The optimal PMF solution had five factors with 20% of extra modeling uncertainty.

Section S3. Calculation of particle-phase liquid water content (LWC_p) and particle acidity (H_p^+).

LWC_p was associated to both organic (LWC_{org}) and inorganic components (LWC_{inorg}) in $PM_{2.5}$. The LWC_{org} was calculated using the following equation:

$$\mathrm{LWC}_{org} = \frac{m_{org}\rho_w}{\rho_{org}}\frac{k_{org}}{(1/RH-1)}$$

where m_{org} is the concentration of organic matter (OM), and in this paper, 1.98 and 1.50 were adopted for OM/OC ratio in the heating and non-heating seasons, respectively (Xing et al., 2013). ρ_w and ρ_{org} are the densities of water and organic, with values of 1 g cm^{-3} and 1.4 g cm^{-3}, respectively (Guo et al,, 2015). k_{org} is the organic hygroscopicity parameter (k_{org}=0.1, Wu et al., 2016), and RH is the relative humidity (%).

Particle acidity (H_p^+) was calculated using the following equation:

$$H_P^+ = \frac{1000H_{air}^+}{LWC_{org}+LWC_{inorg}}$$

where H_p^+ (mol/L) is the concentration of hydronium ion in the aqueous solution, interpreted as particle acidity. H_{air}^+ and LWC_{inorg} were calculated by ISORROPIA- Ⅱ using inorganic ions (Na^+, SO_4^{2-}, NH_4^+, Cl^-, Ca^{2+}, K^+, and Mg^{2+}), RH and temperature as the inputs (Fountoukis and Nenes, 2007).

Table S1. Concentrations of hopanes, levoglucosan, and major aerosol constituents during the heating and non-heating seasons

Species	Heating season			Non-heating season		
	Mean	**Median**	**Range**	**Mean**	**Median**	**Range**
			Hopanes (ng m^{-3})			
17α(H)-22,29,30-trisnorhopane	2.75	2.92	0.46 – 6.45	0.41	0.31	0.15 – 1.10
17α(H),21β(H)-30-norhopane	7.19	6.56	0.97 – 17.1	1.72	1.33	0.44 – 4.95
17α(H),21β(H)-hopane	3.51	3.34	0.85 – 7.64	1.81	1.51	0.53 – 5.83
17α(H),21β(H)-22R-homohopane	0.63	0.55	0.16 – 1.96	0.46	0.38	0.16 – 1.23
17α(H),21β(H)-22S-homohopane	2.94	2.89	0.65 – 6.16	1.34	1.14	0.36 – 3.57
Hopanes (SUM)	17.0	16.6	3.20 – 37.7	5.74	4.91	1.73 – 16.7
			Major Ions (μg m^{-3})			
Sodium	0.55	0.55	0.08 – 1.69	0.27	0.22	0.05 – 0.72
Ammonium	8.84	5.87	0.88 – 34.7	5.02	2.93	0.28 – 22.8
Sulfate	14.7	7.52	2.14 – 59.9	10.5	7.24	0.65 – 38.6
Cloride	3.81	2.97	0.47 –16.1	0.82	0.77	0.05 – 2.85
			Other species			
Levoglucosan (ng m^{-3})	310	251	22.8 – 1188	114	86.3	19.5 – 555
OC (μg m^{-3})	19.1	18.3	4.87 – 40.9	9.77	8.96	3.33 – 29.1
EC(μg m^{-3})	2.61	2.32	0.43 – 5.50	1.53	1.32	0.33 – 3.50

Table S2. Concentrations of individual $HULIS_{WS}$ species during the heating and non-heating seasons

Concentration ($ng\ m^{-3}$)	Heating season			Non-heating season		
	Mean	**Median**	**Range**	**Mean**	**Median**	**Range**
			Individual $HULIS_{WS}$ species			
adipic acid	6.59	3.50	0.91 – 25.5	5.28	4.40	2.01 – 17.7
pimelic acid	2.94	1.77	0.41 -9.57	2.50	2.21	0.86 – 11.5
vanillic acid	5.88	6.32	0.47 – 12.9	1.28	0.60	n.d. – 10.6
azelaic acid	13.7	10.3	1.14 – 35.5	14.9	13.9	3.86 – 55.2
syringic acid	7.04	4.59	0.38 – 16.5	2.08	1.04	0.29 – 16.0
2-hydroxybenoic acid	6.70	5.40	0.71 – 22.4	1.00	0.69	n.d. – 3.26
3-hydroxybenoic acid	6.03	4.96	0.54 – 21.1	1.03	0.76	n.d. – 6.97
4-hydroxybenoic acid	19.3	13.7	0.99 – 57.6	4.39	1.74	0.47 – 63.3
phthalic acid	54.4	25.0	6.55 – 424	22.0	23.8	6.88 – 69.4
isophthalic acid	4.77	3.29	0.64 – 17.8	2.87	2.30	1.06 – 14.9
terephthalic acid	150	97.7	17.0 – 411	98.1	79.6	7.30 – 372
4-nitrophenol	35.1	27.7	1.49 – 105	2.86	1.56	0.45 – 14.5
4-nitrocatechol	27.1	20.6	0.62 – 103	2.91	1.54	0.50 – 28.1
2-hydroxy-5-nitrobenzoic acid	8.50	8.60	0.33 – 23.8	6.38	8.12	0.72 – 15.8
2-methyl-4-nitrophenol	27.2	24.8	1.47 – 56.9	1.91	0.85	0.32 – 9.68
4-methyl-5-nitrocatechol	7.38	7.94	0.26 – 17.6	0.51	n.d.	n.d. – 8.70
3-methyl-6-nitrocatechol	18.6	16.6	0.51 – 54.5	2.25	1.47	n.d. – 13.7
1,2,3-benzenetricarboxylic acid	27.3	12.6	2.24 – 168	16.2	13.2	n.d. – 65.2
1,2,4-benzenetricarboxylic acid	22.7	11.9	1.98 – 114	13.7	11.5	4.09 – 43.3
1,3,5-benzenetricarboxylic acid	5.95	0.98	0.23 – 134	1.35	0.93	0.26 – 4.94
$\Sigma HULIS_{WS\text{-}quantified}$	458	368	39.62– 1657	203	178	41.9 – 782

SOA tracers						
3-hydroxyglutaric acid	3.66	3.50	0.36 – 9.77	1.81	1.84	0.71 – 4.85
3-acetylpentanedioic acid	2.47	1.71	n.d. – 8.40	4.44	3.83	1.16 – 10.33
3-hydroxy-4,4-dimethylglutaric acid	1.06	0.80	n.d. – 3.01	1.16	1.04	0.37 – 3.11
3-Isopropylpentanedioic acid	4.01	3.34	n.d. – 14.09	5.34	5.11	1.02 – 11.80
3-methyl-1,2,3-butanetricarboxylic acid	1.26	1.05	n.d. – 3.30	4.09	3.15	1.09 – 9.80

n.d.: not detected.

Table S3. Multilinear regression analysis of PMF-resolved $HULIS_{WS}$ from vehicle emissions ($HULIS_{WS\_VE}$), particle acidity (H_p^+), particle-phase liquid water content (LWC_p), and particle-phase SO_4^{2-}, NO_X and O_3

Variable	β-coefficient	Standard error	t value	*p* value
Intercept	0.337	0.220	1.530	0.131
H_p^+	-0.113	0.508	-0.223	0.824
LWC_p	-0.008	0.008	-0.972	0.335
SO_4^{2-}	0.018	0.013	1.381	0.172
NO_X	0.012	0.003	4.254	0.000
O_3	-0.013	0.004	-3.008	0.004

Table S4. Multilinear regression analysis of PMF-resolved $HULIS_{WS}$ from secondary aerosol formation ($HULIS_{WS\_SEC}$), particle acidity (H_p^+), particle-phase liquid water content (LWC_p), and particle-phase SO_4^{2-}, NO_X and O_3

Variable	β-coefficient	Standard error	t value	*p* value
Intercept	-0.031	0.357	-0.088	0.930
H_p^+	1.291	0.822	1.571	0.121
LWC_p	0.026	0.013	1.997	0.050
SO_4^{2-}	0.066	0.021	3.227	0.002
NO_X	-0.001	0.005	-0.267	0.790
O_3	0.028	0.007	3.942	0.000

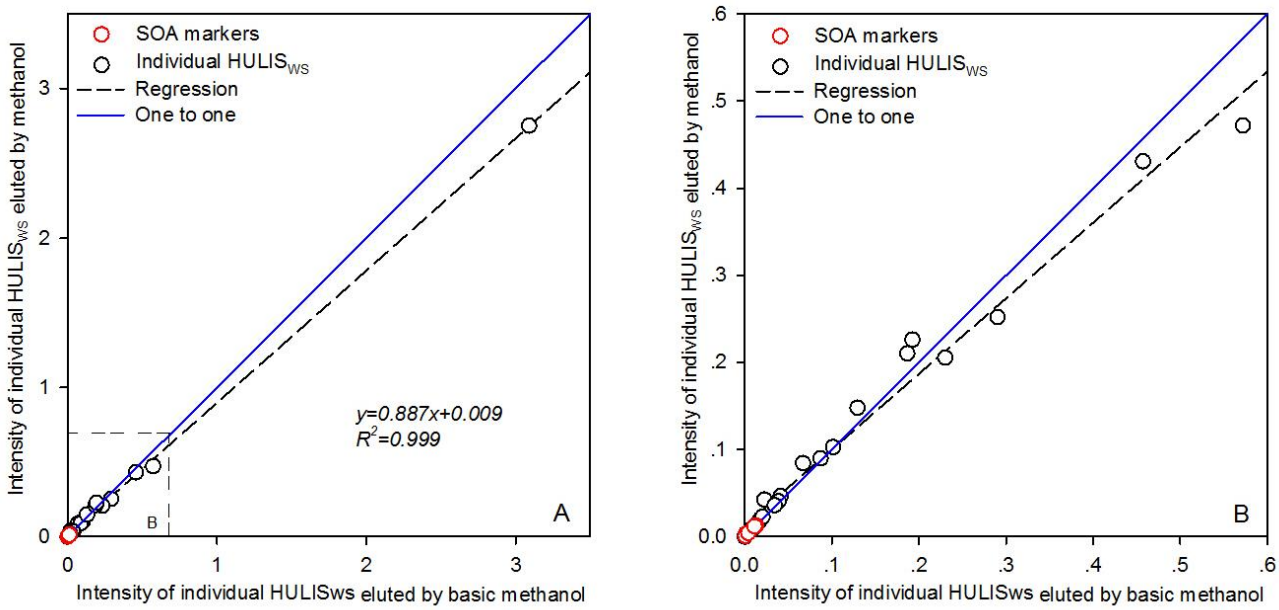

Figure S1. Comparison of GC-MS peak intensities of $HULIS_{WS}$ species eluted by methanol and basic methanol (panel B is the magnification of panel A with the intensity below 0.6)

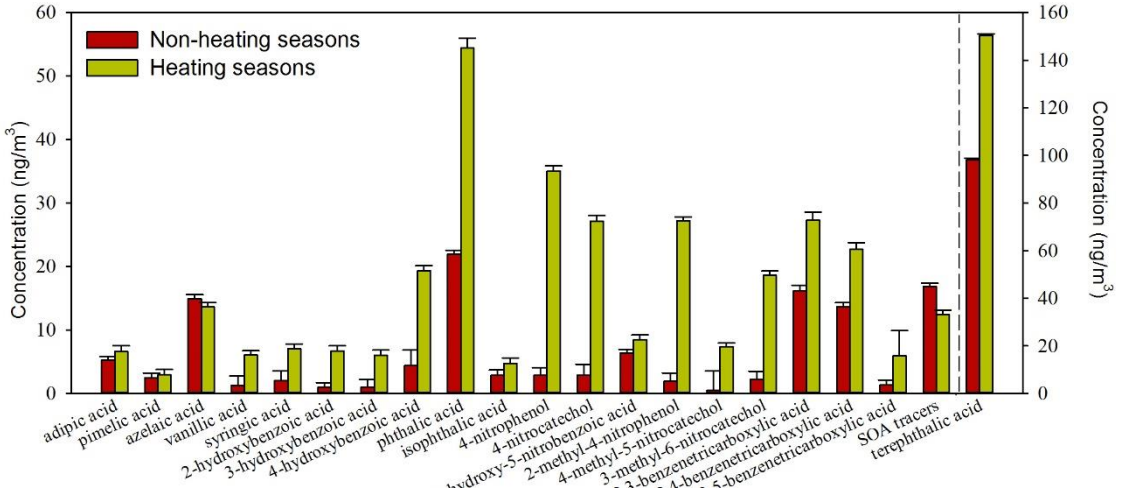

Figure S2. Comparison of concentration levels of individual $HULIS_{WS}$ species in the heating and non-heating seasons.

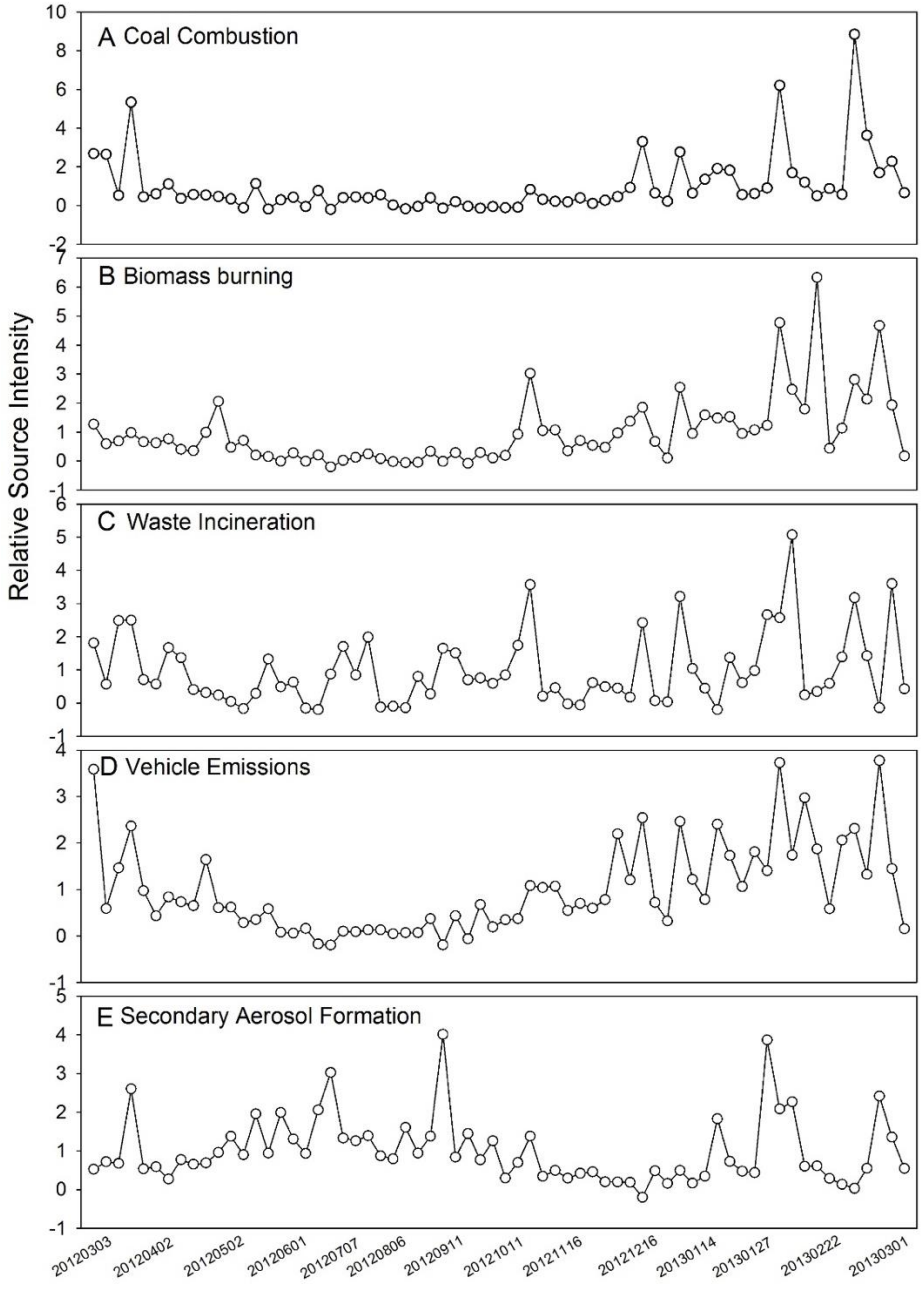

Figure S3. Relative source intensities of PMF source profiles.

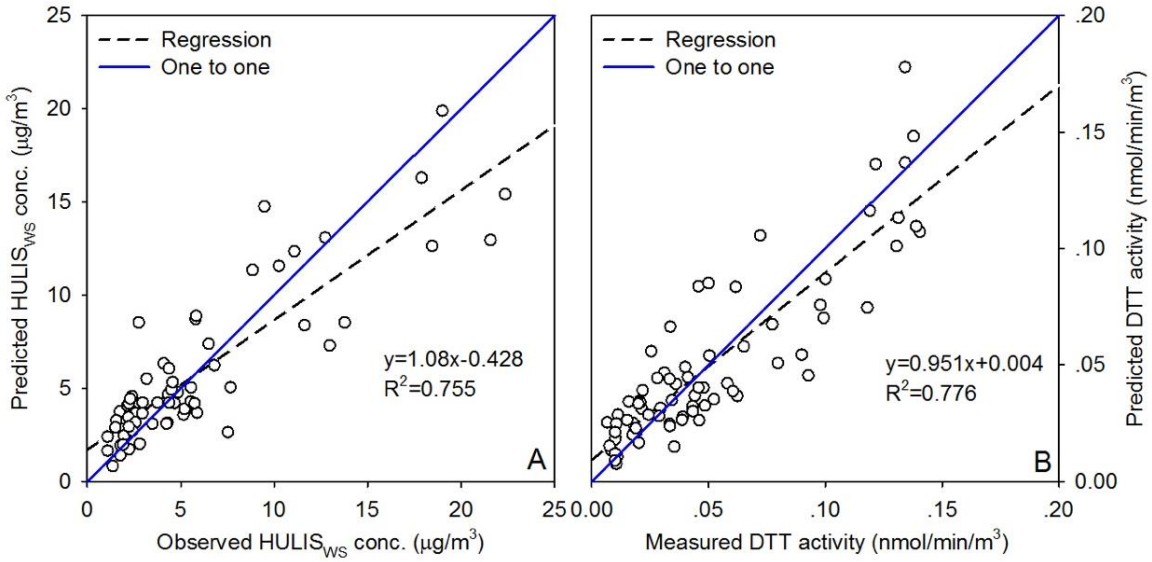

Figure S4. PMF-predicted versus measured concentrations of HULIS$_{WS}$ mass concentration (panel A) and extrinsic DTT activity of HULIS$_{WS}$ (panel B).

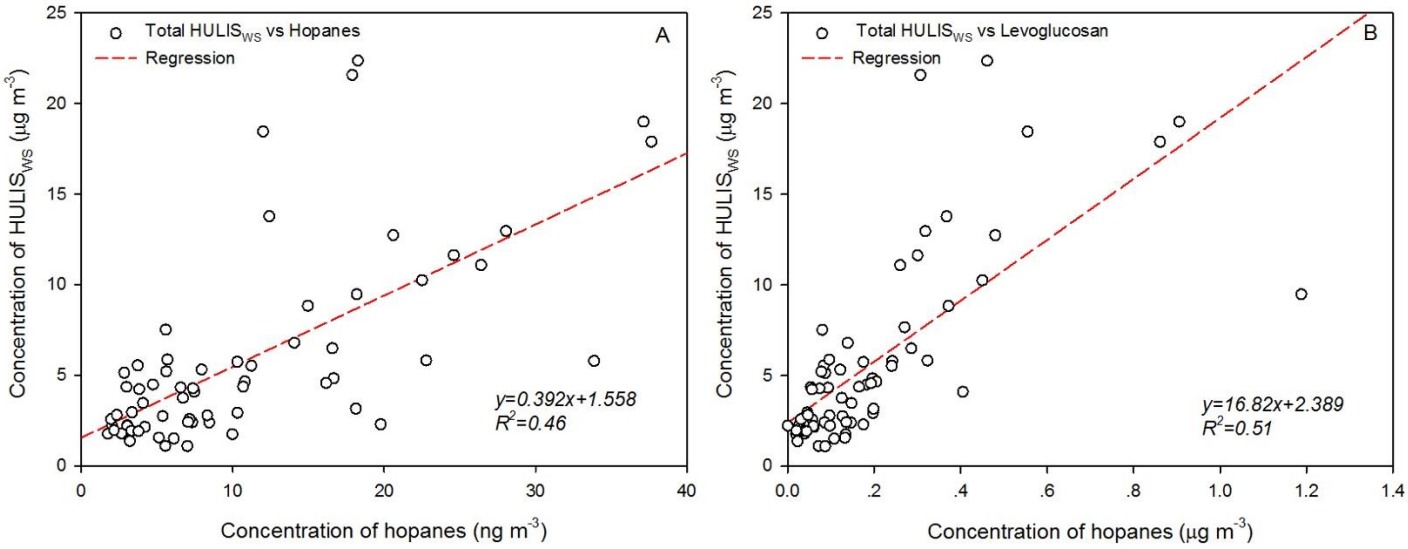

Figure S5. HULIS$_{WS}$ mass concentration versus hopanes (panel A) and levoglucosan (panel B)

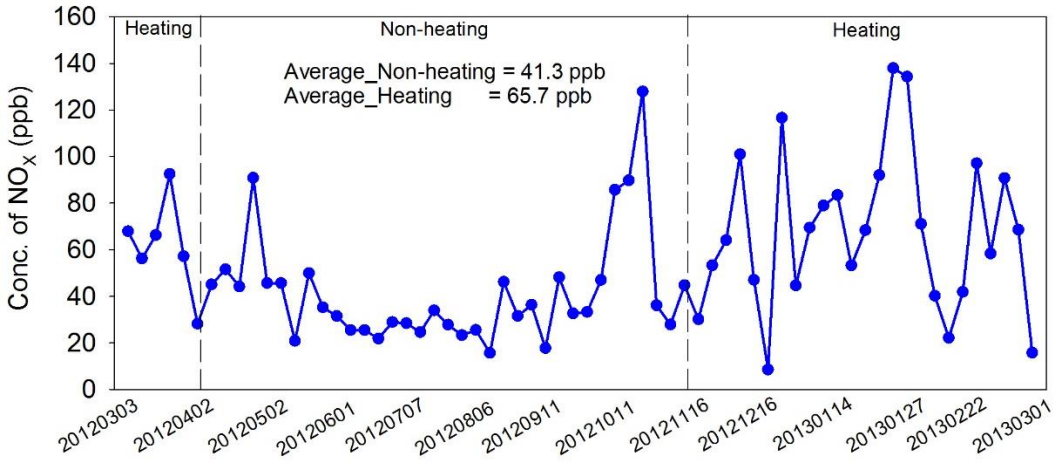

Figure S6. Temporal variation for gas-phase NO$_X$ concentration in Beijing during 2012-2013.

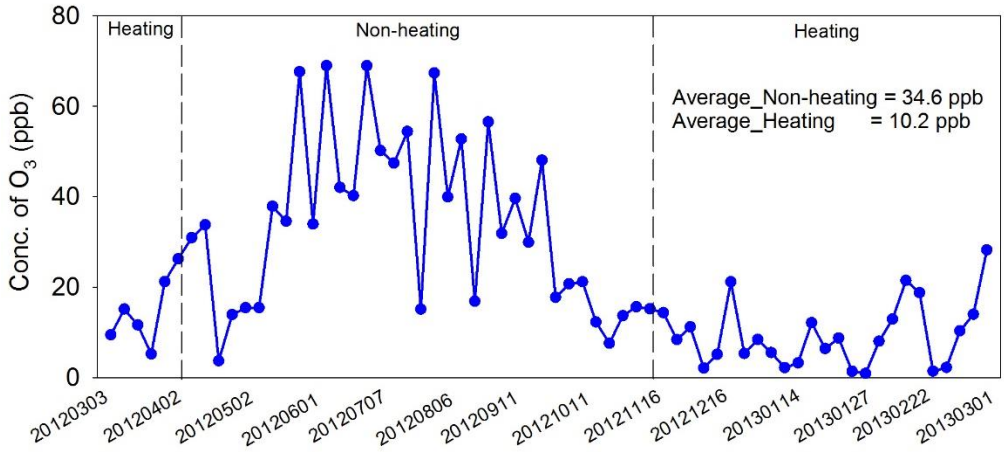

Figure S7. Temporal variation for gas-phase O_3 concentration in Beijing during 2012-2013.

References:

Fountoukis, C. and Nenes, A.: ISORROPIA II: a computationally efficient thermodynamic equilibrium model for K–H_2O aerosols, Atmos. Chem. Phys., 7, 4639–4659, 2007.

Guo, H., Xu, L., Bougiatioti, A., Cerully, K. M., Capps, S. L., Hite, J. R., Carlton, A. G., Lee, S. H., Bergin, M. H., Ng, N. L., Nenes, A. and Weber, R. J.: Fine-particle water and pH in the southeastern United States, Atmos. Chem. Phys., 15(9), 5211–5228, 2015.

Hu, D., Bian, Q., Li, T. W. Y., Lau, A. K. H. and Yu, J. Z.: Contributions of isoprene, monoterpenes, β-caryophyllene, and toluene to secondary organic aerosols in Hong Kong during the summer of 2006, J. Geophys. Res. Atmos., 113(22), D22206, 2008.

Hu, D., Bian, Q., Lau, A. K. H. and Yu, J. Z.: Source apportioning of primary and secondary organic carbon in summer $PM_{2.5}$ in Hong Kong using positive matrix factorization of secondary and primary organic tracer data, J. Geophys. Res. Atmos., 115(16), 1–14, 2010.

Lin, P., Huang, X. F., He, L. Y. and Zhen Yu, J.: Abundance and size distribution of HULIS in ambient aerosols at a rural site in South China, J. Aerosol Sci., 41(1), 74–87, 2010.

Wu, Z. J., Zheng, J., Shang, D. J., Du, Z. F., Wu, Y. S., Zeng, L. M., Wiedensohler, A. and Hu, M.: Particle hygroscopicity and its link to chemical composition in the urban atmosphere of Beijing, China, during summertime, Atmos. Chem. Phys., 16(2), 1123–1138, 2016.

Xing, L., Fu, T. M., Cao, J. J., Lee, S. C., Wang, G. H., Ho, K. F., Cheng, M. C., You, C. F. and Wang, T. J.: Seasonal and spatial variability of the OM/OC mass ratios and high regional correlation between oxalic acid and zinc in Chinese urban organic aerosols, Atmos. Chem. Phys., 13(8), 4307–4318, 2013.